RESEARCH ARTICLE

The effect and efficiency of attentional networks and the brain electrophysiology

Hossein Akbari-Lalimi[1] · Shahrokh Naseri[1] · Mahdi Momennezhad[2] · Hoda Zare[1,3] · Ali Talaei[4] · Seyed Ali Shafiei[5]

Abstract

The attention networks test (ANT) is frequently utilized to evaluate executive, alerting, and orienting attentional components. Additionally, it serves as an activation task in neuroimaging studies. This study aimed to examine the relationship between attention networks and brain electrophysiology. The study enrolled 40 right-handed male students (age $= 20.8 \pm 1.3$ years) who underwent the revised attention network test, while their electroencephalogram signals were recorded. The study aimed to explore the effects of attention networks and their efficiencies on brain electrophysiology. The results indicated that the P3 amplitude was modulated by the conflict effect in the central (p-value $= 0.014$) and parietal (p-value $= 0.002$) regions. The orienting component significantly influenced P1 and N1 latencies in the parietal and parieto-occipital regions (p-values < 0.006), as well as P1 and N1 amplitude in the parieto-occipital region (p-values $= 0.017$ and 0.011). The alerting component significantly affected P1 latency and amplitude in the parietal and parieto-occipital regions, respectively (p-value $= 0.02$). Furthermore, N1 amplitude and the time interval between P1 and N1 were significantly correlated with the efficiency of alerting and orienting networks. In terms of connectivity, the coherence of theta and alpha bands significantly decreased in the incongruent condition compared to the congruent condition. Additionally, the effects of attention networks on event-related spectral perturbation were observed. The study revealed the influence of attention networks on various aspects of brain electrophysiology. Specifically, the alerting score correlated with the amplitude of the N1 component in the double-cue and no-cue conditions in the parieto-occipital region, while the orienting score in the same region correlated with the N1 amplitude in the valid cue condition and the difference in N1 amplitude between the valid cue and double-cue conditions. Overall, empirical evidence suggests that attention networks not only impact the amplitudes of electrophysiological activities but also influence their time course.

Keywords Attention · Alerting · Orienting · Executive · Event-related potential

Communicated by Bill J Yates.

✉ Seyed Ali Shafiei
sashafiei@muq.ac.ir; salishafiei@yahoo.com

1 Department of Medical Physics, Faculty of Medicine, Mashhad University of Medical Sciences, Mashhad, Iran

2 Nuclear Medicine Research Center, Mashhad University of Medical Sciences, Mashhad, Iran

3 Medical Physics Research Center, Mashhad University of Medical Sciences, Mashhad, Iran

4 Psychiatry and Behavioral Sciences Research Center, Mashhad University of Medical Sciences, Mashhad, Iran

5 Neuroscience Research Center, Qom University of Medical Sciences, Qom, Iran

Introduction

The attention network test (ANT) was introduced to evaluate three components of attention based on the Posner attention model (Fan et al. 2002). According to this model, attention is divided into three networks: alerting, orienting, and executive network. The ANT combines spatial cue (Posner 1980) and flanker (Eriksen and Eriksen 1974) tasks, requiring subjects to choose the direction of a target arrow surrounded by four arrows. The efficiency of each attention component is calculated by comparing reaction times across different target and cue conditions. Furthermore, this task serves as an activation task in neuroimaging studies.

Furthermore, the impact of attention and its associated networks on brain activity has been examined in various studies, revealing distinct patterns in event-related potential

(ERP) waveforms that distinguish the effects of different attention networks. Some studies have found that the amplitude of the P3 component varies across different congruency conditions, with the incongruent condition leading to a reduction in P3 amplitude in the parietal region compared to the congruent condition (Galvao-Carmona et al. 2014; Gonçalves et al. 2018; Kaufman et al. 2016; Neuhaus et al. 2011, 2010; Williams et al. 2016). Additionally, different cue conditions associated with alerting and orienting networks have been found to modulate the target-locked N1 and P1 components in the parietal and occipital areas (Galvao-Carmona et al. 2014; Gonçalves et al. 2018; Kaufman et al. 2016; Neuhaus et al. 2010; Racer et al. 2011; Williams et al. 2016). Regarding alerting, the amplitude of the target-locked P1 component was found to be higher in the no-cue condition compared to the double-cue condition in one study (Gonçalves et al. 2018). However, this effect was not observed in another study (Galvao-Carmona et al. 2014), as the amplitude of the target-locked P1 component did not differ between the no-cue and central cue conditions. Moreover, the amplitude of the target-locked N1 component was found to be higher in the central cue and double-cue conditions compared to the no-cue condition (Galvao-Carmona et al. 2014; Gonçalves et al. 2018). Furthermore, spatial cue conditions were elicit faster N1 latencies compared to the no-cue condition (Galvao-Carmona et al. 2014). Regarding the orienting, the amplitude of target-locked N1 in a study (Gonçalves et al. 2018) is higher in the spatial cue condition than in the central cue condition, while in another study (Galvao-Carmona et al. 2014), it is lower. The N1 delay was also investigated, demonstrating that the spatial cue condition is faster than the central cue condition in the congruent target condition (Galvao-Carmona et al. 2014). Additionally, the amplitude of the target-locked P1 in the spatial cue condition is higher than that in the central cue condition in the parieto-occipital region (Galvao-Carmona et al. 2014; Gonçalves et al. 2018).

The effect of attention networks on brain electrophysiology has been investigated in previous studies. These studies have observed significant effects of all three attention networks on event-related potential (ERP) components. However, the results of these studies are not entirely consistent with each other when it comes to the effect of attention networks on ERP components. Additionally, the correlation between the efficiency of attention networks and brain ERP components has not been investigated in previous surveys. Furthermore, the differences in functional brain connectivity, event-related desynchronization (ERD), and event-related synchronization (ERS) for each pair of conditions corresponding to each attention network can provide valuable new insights. Therefore, the objective of the present study is to investigate the relationship between attentional networks and their efficiency in terms of brain

electrophysiology. This will be examined through the analysis of ERP, event-related spectral perturbation (ERSP), and functional connectivity.

Materials and methods

Samples

In the present study, a total of 40 healthy young males (age = 20.8 ± 1.3 years; all right-handed) were included from university students. None of them were under the influence of alcohol or drugs. This study was approved by the Ethics Committee of Mashhad University of Medical Sciences.

EEG data collection

The EEG signal was recorded using a 10–20 international system with 32 active electrodes and one reference electrode on the right ear. The recording was conducted using a g.HIamp amplifier (g.tec, Austria). The ground electrode was positioned on the frontal part (Fpz), and the sampling frequency was set to 512 Hz. During the preparation phase, all channels were visually inspected for any noise, and the electrodes were required to have a maximum resistance of 50 kΩ. The appearance time of the stimuli, the types of different stimuli used in the task, and the time and type of the subject's response were recorded simultaneously and synchronously with the EEG signal using the parallel port and g.TRIGbox system (g.tec, Austria). During the recording of certain samples, the EEG signal was captured using a 32-channel amplifier of the g.USBamp (g.tec, Austria), instead of the g.HIamp (g.tec, Austria), resulting in the recording of 29 EEG channels.

Revised attention network test (ANT-R)

ANT-R, which was presented by Fan et al., served as the basis for the current study (Fan et al. 2009). The revised attention network test encompasses the same attention-related networks and mechanisms as the original test. Additionally, it introduces new features, such as the variable cue-target interval, which eliminates the influence of predictability regarding the exact timing of target stimulus presentation. The experiment took place in the National Brain Mapping Laboratory, within a quiet and dimly lit room. The EEG signal was simultaneously recorded alongside the performance of the task. Stimuli presentation and response recording were accomplished using the Psychtoolbox (Kleiner et al. 2007). This toolbox serves as an interface between the computer hardware and MATLAB software (MathWorks, Natick, MA, USA). The task design included three types of cues (no cue, double cue, and spatial cue)

and two congruency conditions (congruent and incongruent). The nominal frequency of the monitor used for the task presentation was 60 Hz, and the distance between the subject's eyes and the screen was maintained at 60 cm. Participants were instructed to read the task instructions and seek clarification if needed.

The details of the task used in this study are depicted in Fig. 1. The task consists of a fixed cross positioned at the center of the screen, which is presented against a gray background. Two rectangular boxes are positioned on either side of the cross. During trials with a cue, either one or both of the boxes flash for a duration of 100 ms. In the absence of a cue, the boxes remain unchanged. Following a variable time interval (randomly selected to be either 0, 400, or 800 ms, with an average of 400 ms), a set of five arrows appears side by side as the target stimuli. These arrows are displayed for a duration of 500 ms. Within each trial, the target stimulus appears within one of the right or left boxes. Participants are required to identify and select the direction of the middle arrow. In the congruent condition, all five arrows point in the same direction, whereas in the incongruent condition, the direction of the four flanker arrows opposes the direction of the central arrow. The time intervals between trials vary from 2000 to 12,000 ms, with an average interval of 4000 ms. The average duration of each trial is 5000 ms, and a window of 1700 ms is considered for subjects to respond.

The task consists of four blocks, each containing 60 trials, resulting in a total of 240 trials. Half of the trials are congruent, while the other half are incongruent. Additionally, out of the 240 trials, 40 are conducted without cues, 40 include double cues providing temporal information, and 160 trials include spatial cues providing spatiotemporal information. Within the 160 trials with spatial cues, 120 trials have valid cues, while the remaining 40 trials involve invalid cues.

Processing and calculation of cognitive functions

In order to assess the performance of each attention network, the initial 40 trials of each subject were omitted. This decision was made to eliminate any learning bias from the study. To determine the alerting score, the difference in reaction time between the no-cue and double-cue conditions was measured. The orienting score was obtained by calculating the reaction time difference between the double-cue and valid spatial cue conditions. The executive score was computed as the reaction time difference between the incongruent and congruent conditions:

$$Alerting = RT_{no\ cue} - RT_{double\ cue},$$

$$Orienting = RT_{double\ cue} - RT_{valid\ cue},$$

$$Executive = RT_{incongruent} - RT_{congruent}.$$

Signal analysis

The signal analysis of EEG was conducted using the EEGLAB (Delorme and Makeig 2004), ERPLAB (Lopez-Calderon and Luck 2014), and FieldTrip (Oostenveld et al. 2011) toolboxes in MATLAB 2018b. Figure 2 presents the flowchart of the EEG signal processing pipeline. EEG data
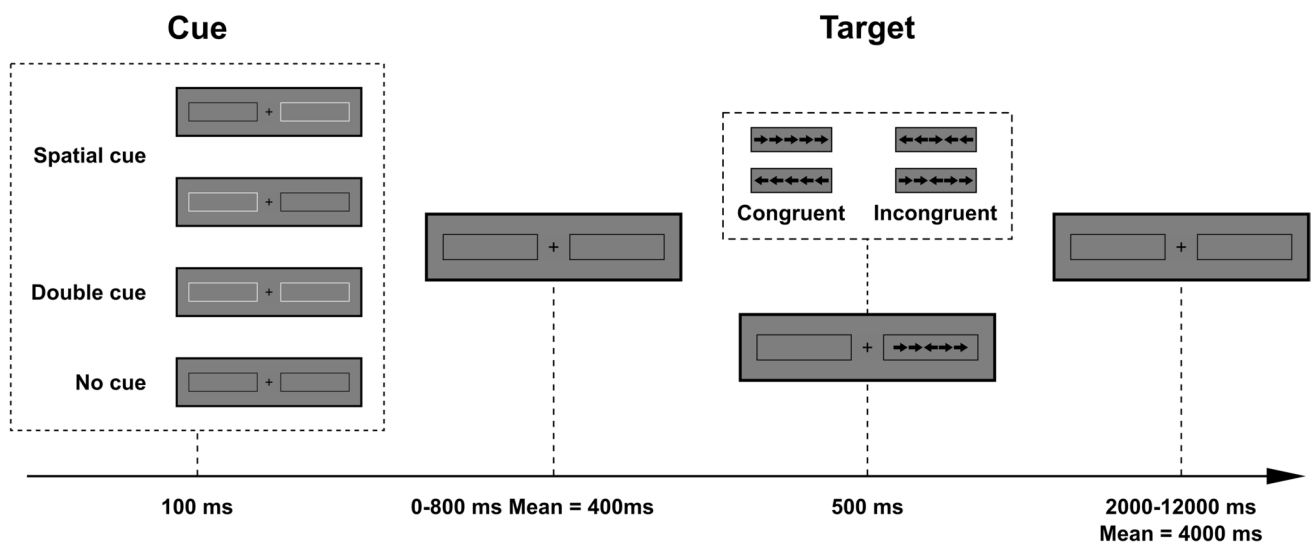

Fig. 1 The schematic of the revised attention network test. Five arrows, whether congruent or incongruent, are presented on either the left or right side of the screen. These arrows are displayed for a duration of 500 ms after a variable interval. Before the presentation of the target stimuli, three possible cue conditions may occur. Subsequently, participants are then tasked with selecting the direction of the central arrow. The duration of the inter-trial interval ranges from 2000 to 12,000 ms.
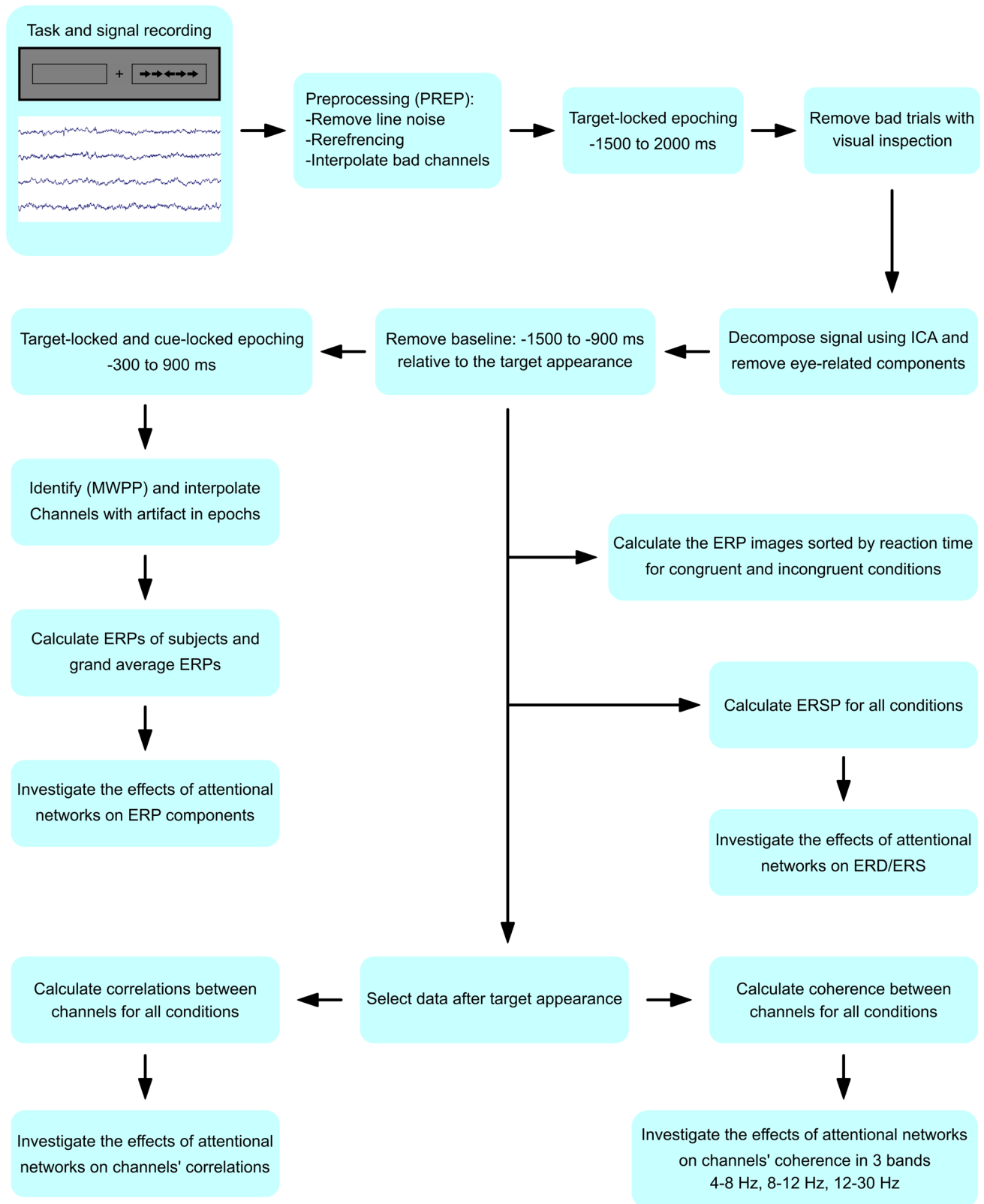
Fig. 2 Diagram of EEG signal analysis pipeline

preprocessing was performed based on the PREP pipeline (Bigdely-Shamlo et al. 2015). In summary, the line noise was removed without committing to a filtering strategy, the signal was robustly re-referenced relative to an estimate of the true average reference, and the bad channels relative to this reference were detected and interpolated (median = 3.5 and IQR = 2). Subsequently, the signal was epoched relative to the time of the appearance of the target stimuli in the range of − 1500 to 2000 ms. During visual inspection, trials with high noise were excluded for each sample. Ultimately, 94.8 ± 4.4% of trials remained after removal.

The signals from the remaining trials were decomposed into independent components using the Independent Component Analysis (ICA) function available in EEGLAB. To identify and remove eye-related components, IClabel (Pion-Tonachini et al. 2019) was utilized. Subsequently, all epochs were baseline-corrected by subtracting the average amplitude within the range of − 1500 to − 900 ms, relative to the target stimulus. For trials with correct responses, ERPLAB was employed to epoch the data based on the onset of the target stimuli and the cue within the timeframe of − 300 to 900 ms.

The epoching process was performed according to the appearance time of target stimuli across five conditions. These conditions consisted of two congruent and incongruent conditions, as well as three conditions categorized as no cue, valid spatial cue, and double cue. The epoching process, which was based on the appearance of the cue, was carried out in the three conditions of no cue, valid spatial cue, and double cue. To identify channels with artifacts within the epochs, the moving window peak-to-peak (MWPP) algorithm was utilized. Channels exhibiting artifacts were subsequently interpolated in the corresponding epochs (median = 0.65% and IQR = 1.4%). Lastly, the ERP (event-related potential) was calculated for each individual by averaging the epochs. Furthermore, the grand average ERP was computed by averaging the ERP of all subjects.

In addition to event-related potentials, event-related spectral perturbation was also calculated to investigate event-related synchronization and event-related desynchronization. To conduct this analysis, the EEGLAB toolbox was utilized. The processing of the EEG signals up to the baseline correction stage was identical to that of the event-related potentials calculation. Subsequently, the EEGLAB toolbox was employed to estimate the changes in power spectrum during epoch periods, within the frequency range of 4–40 Hz, for various conditions in each subject. These estimates were then averaged across subjects.

Also, the EEG connectivity analysis was conducted to evaluate the relationship between pairs of EEG signals recorded from different channels. In this study, two connectivity metrics were compared for each pair of conditions associated with each network using the FieldTrip toolbox:

correlations of time series and spectral coherence. For connectivity analysis, such as ERSP analysis, the baseline-corrected EEG signals were utilized. Subsequently, the EEG signals after the appearance of the target stimulus were selected in the epochs corresponding to the two congruency conditions and the three cue conditions. On the one hand, the correlation between the signals of the channels was calculated, and on the other hand, the coherence between the channels was calculated after determining the power spectrum of the channels. The coherence was calculated in three frequency bands: 8–4 Hz, 12–8 Hz, and 12–30 Hz. Consequently, the EEG connectivity analysis yielded four connectivity matrices for each subject and each condition

Statistical analysis

The amplitude and latency of the target-locked P3 were compared between congruent and incongruent conditions in the Pz and Cz channels. Additionally, the amplitude and latency of the target-locked P1 and N1 components, as well as the difference between these components, were compared between the double-cue and no-cue conditions and between the valid and double-cue conditions in the parietal and parieto-occipital regions. Furthermore, the amplitude and latency of the cue-locked P1 and N1 components, along with the differences between these components, were calculated and compared between the double-cue and no-cue conditions, as well as between the valid cue and double-cue conditions in the parieto-occipital and occipital regions. The correlation between the target-locked P3 components in the central and parietal regions and the executive network was investigated. Moreover, the correlations of the target-locked P1 and N1 components with the alerting and orienting networks in the parietal and parieto-occipital regions were examined. The selection of regions to investigate the effect of attention networks was based on previous literature (Galvao-Carmona et al. 2014; Kaufman et al. 2016; Neuhaus et al. 2011, 2010; Williams et al. 2016).

A p-value of < 0.05 was considered as a significant threshold for examining the presence of a significant difference between means or the presence of a significant correlation in statistical analysis. The r index, also known as the correlation coefficient, was employed to assess the effect size in correlation, while Cohen's d index, calculated as the difference between means divided by the overall standard deviation, was utilized to assess the effect size in mean difference.

Also, ERP images corresponding to conditions related to the calculation of attention network scores were plotted. In these images, the trials were sorted based on reaction time to represent the relationship between attention network scores and reaction time, as well as the variation over single trials and temporal diversion.

To investigate the effect of attentional networks on ERD/ERS, event-related spectral perturbation was compared between different cue and target conditions associated with each network. All conditions were target-locked. A *p*-value of < 0.05 was considered as a significance threshold to analyze the impact of each network on the ERD/ERS pattern. The Bonferroni method was employed to address the issue of multiple hypothesis testing.

To evaluate the impact of attentional networks on brain connectivity, we compared connectivity matrices for different cues and target conditions associated with each network. A *p*-value below 0.05 was regarded as a significant threshold to explore the effect of each network on brain connectivity. In order to address the issue of multiple comparisons in the connectivity matrices, we employed various correction methods including Bonferroni, false discovery rate (FDR) 10%, and Hochberg approaches, as described by Menyhart et al. (2021).

Results

Behavioral efficiency

The mean reaction time of the subjects was 689 ± 92 ms, and the mean error rate was $4.9\% \pm 3.3\%$. Regarding the efficiency of the attention networks, the effect of alerting was 56 ± 48 ($t(39) = 7.39$, Cohen's $d = 1.2$, *p*-value < 0.0001), the effect of orienting was 48 ± 35 ($t(39) = 8.53$, Cohen's $d = 1.4$, *p*-value < 0.0001), and the effect of executive was 121 ± 31 ($t(39) = 24.4$, Cohen's $d = 3.9$, *p*-value < 0.0001). The data from one participant were excluded from further analysis due to considerable differences in accuracy and reaction time compared to the group, exceeding three standard deviations.

Congruency P3

Figure 3 illustrates the voltage distribution map on the scalp for both congruent and incongruent conditions, as well as the difference between these two conditions during the time
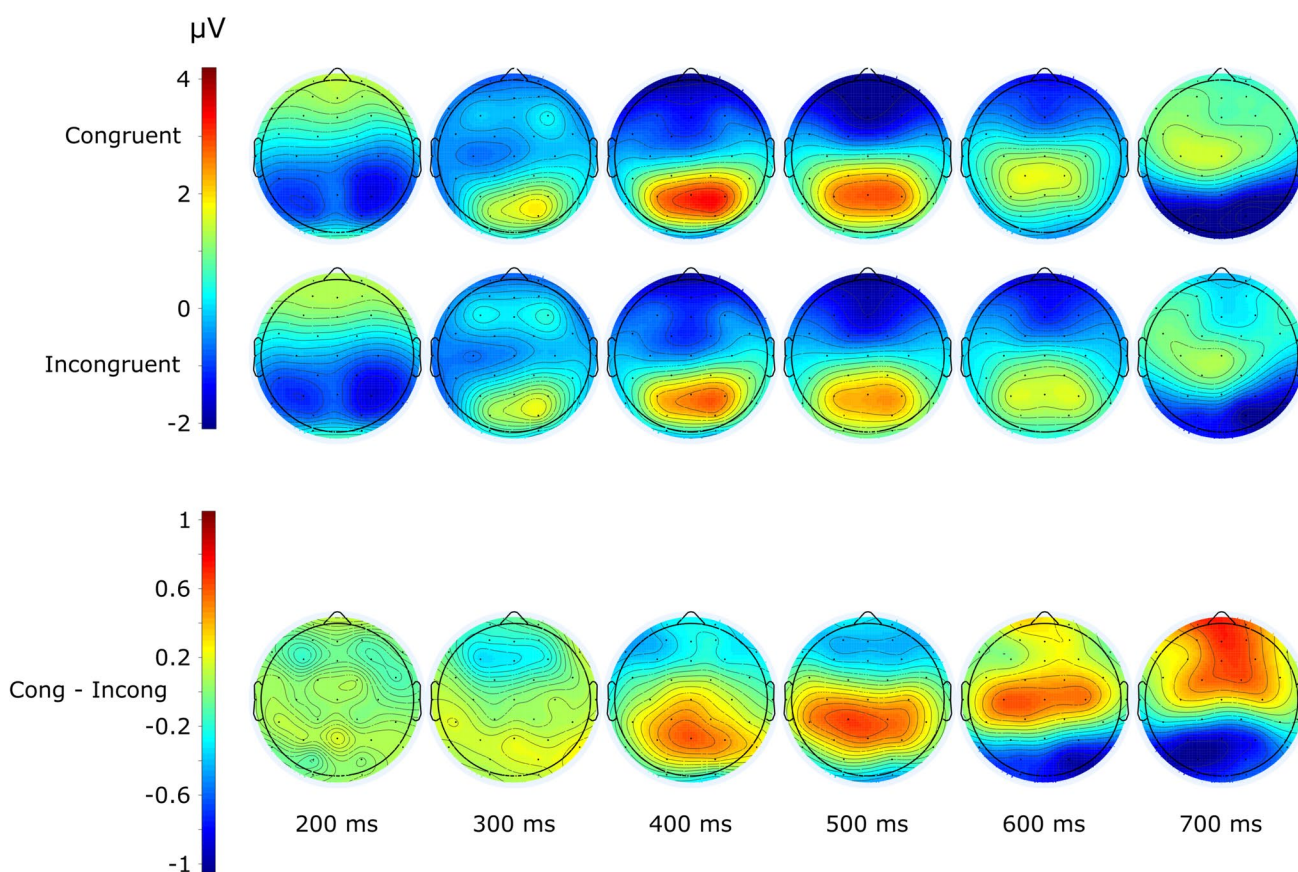

Fig. 3 2D EEG activity topographic voltage maps by target condition. The top row represents the congruent condition, the middle row represents the incongruent condition, and the bottom row represents the difference between these two conditions. Notably, in the 400–600 ms time window, considerable differences between the congruent and incongruent conditions were observed in the parietal and central regions

interval of 200–700 ms after the target stimulus appears. Meanwhile, Table 1 presents the average amplitude of the P3 peak in the Pz channel (a local maximum within the range of 300–600 ms) and the average P3 amplitude in the Cz channel (mean value of the signal within the range of 350–700 ms) for the congruent and incongruent target conditions. It was found that the parietal P3 peak amplitude following congruent targets was significantly higher compared to the peak amplitude following incongruent targets. Similarly, within the central region, the average P3 amplitude following congruent targets was significantly higher compared to the average amplitude following incongruent targets.

Figure 4 depicts the grand average ERP waveform in Cz and Pz electrodes, representing various congruency conditions based on the timing of the target stimulus appearance. Upon comparing the peak latency of congruent and incongruent conditions in each electrode, no significant difference was observed. Although the congruent conditions exhibited higher peak amplitude and mean amplitude of P3 in the Pz and Cz electrodes compared to the incongruent conditions, there was no significant difference in the area under the curve divided by the distance between the two zero-crossing points.

Table 1 Target-locked P3 amplitude (μV) by target conditions and electrodes

	Con amp (SD)	Incon amp (SD)	*p* (Cohen's *d*)
Pz peak Amp	4.15 (1.88)	3.63 (1.43)	0.002 (0.31)
Cz mean Amp	0.70 (0.81)	0.37 (0.93)	0.014 (0.37)

SD standard deviation

Figure 5 shows the ERP images sorted according to the reaction time in the congruent and incongruent conditions at the Pz channel. A one-tailed *F*-test, following the removal of outliers, demonstrated that the time interval between the reaction time and the P3 component exhibits significantly greater variation in the incongruent condition compared to the congruent condition (*p*-value = 0.038). Additionally, according to Fig. 6, the standard deviation of reaction time and the time interval between the reaction time and P3 latency at the Pz channel were observed to be significantly higher in the incongruent condition than in the congruent condition, with *p*-values of 0.00005 and less than 0.00001, respectively.

Cue type target-locked P1 and N1

Figure 7 displays the target-locked grand average event-related potential (ERP) waveform related to the mean of P3 and P4 electrodes, as well as the mean of PO3 and PO4 electrodes, for different cues. The mean peak amplitude of P1 and N1, along with their associated latencies in the parietal and parieto-occipital regions, is presented in Table 2. The alerting effect was found to be significant in the P1 latency and amplitude in the parietal and parieto-occipital regions, respectively. Additionally, the alerting effect was significant in the P1–N1 amplitude in the parieto-occipital region. Significant effects of the orienting were observed in the latency of the P1 component in the parietal region, as well as the amplitudes and latencies of both the P1 and N1 components in both the parietal and parieto-occipital regions. Furthermore, significant differences in the amplitudes of the P1 and
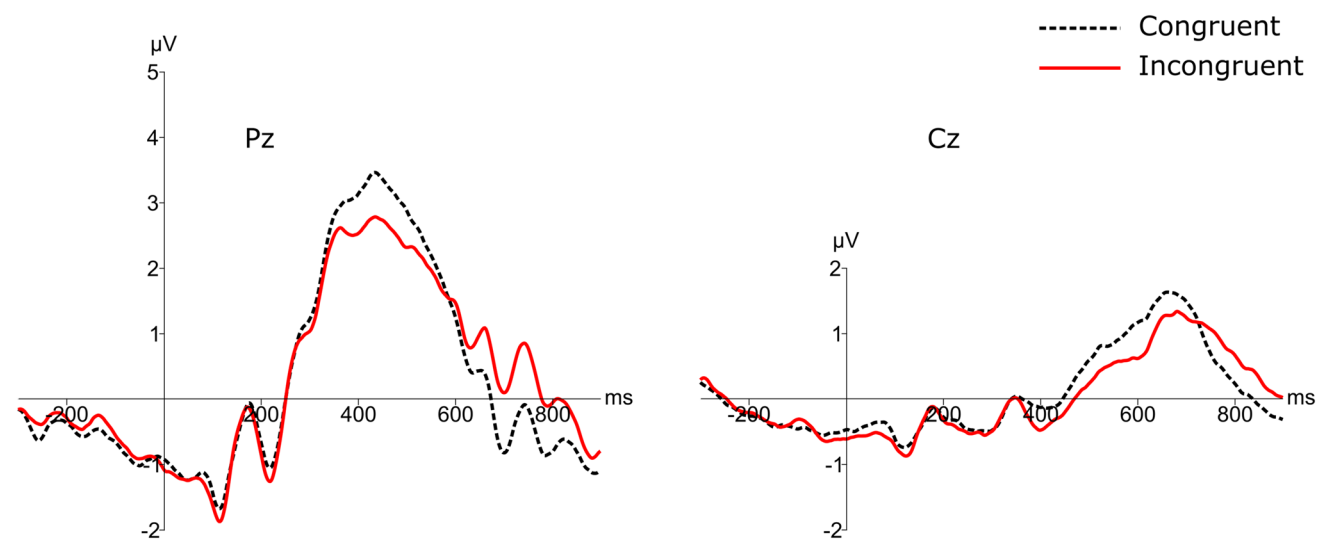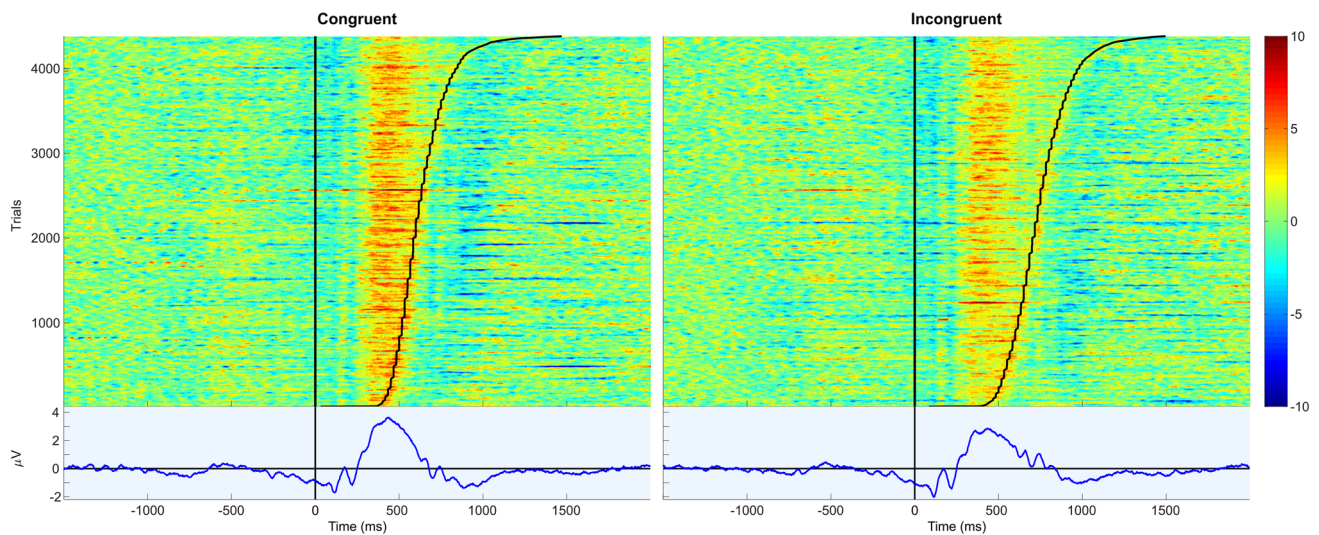

Fig. 4 ERP waveforms along the Pz (left) and Cz (right) electrodes. The ERPs are shown for congruent (dash line) and incongruent (solid line) conditions. In both Pz and Cz channels, the amplitude of P3 in the incongruent condition was significantly lower than in the congruent condition

Fig. 5 The ERP images sorted based on the reaction time in different congruency conditions at the Pz channel. The time interval between the reaction time of subjects and the P3 component has more variation in the incongruent condition significantly

N1 components were observed in the parietal and parieto-occipital regions.

The event-related potential (ERP) images of cue conditions, which are associated with the scores of the alerting and orienting networks (no cue, double cue, and valid cue), are displayed in Fig. 8 at the P3 channel location. The correlations between ERP components and reaction time in different conditions are investigated below.

Cue-locked N1

Figure 9 illustrates the cue-locked grand average ERP waveform related to the average measurements obtained from the O2 and O1 electrodes, as well as those from the PO3 and PO4 electrodes. These measurements were taken under different cue conditions. Table 3 presents the mean N1 peak amplitudes observed in the occipital and parieto-occipital regions. In both areas, the N1 amplitude was higher in the double-cue condition than that in the valid spatial cue condition and greater in the valid spatial cue condition than that in the no-cue condition.

The correlation of the attention networks scores with the ERP component

The correlation between the executive network score and the P3 peak amplitude in the Pz electrode, the average P3 amplitude in the Cz electrode relative to the time of target stimuli appearance in both congruent and incongruent conditions, and the difference between these two conditions were calculated. No significant correlation was observed between these ERP components and the executive network.

Table 4 presents the correlations between the alerting network score and various factors such as the amplitude and latency of P1 and N1 peaks, as well as the difference between these peaks in relation to the time of target stimulus appearance in the parietal and parieto-occipital regions. These correlations are examined in two conditions: no cue and double cue, along with the difference between these conditions. In the parieto-occipital region, the N1 amplitude in both the no-cue and double-cue conditions and the P1 and N1 latency differences (the P1 and N1 interval) in the double cue condition exhibit significant correlations with the alerting network score.

Table 5 presents a summary of the correlations between the score of the orienting network and the amplitude and latency of the P1 and N1 peaks, as well as the difference between these peaks in the target-locked situation. These correlations were examined in the parietal and parieto-occipital regions within both the valid cue and double cue conditions. Furthermore, the difference between these two conditions was also considered. In the double-cue condition and the valid spatial cue condition minus the double-cue condition, significant correlations were observed between the N1 amplitudes in the parieto-occipital region and the orienting network score.

Event-related spectral perturbation

Figure 10 shows the results of event-related spectral perturbation analysis conducted on the alerting network within the parietal and parieto-occipital regions. The results indicate that appearance of the target stimulation and the subject's subsequent response in both the no-cue and double-cue
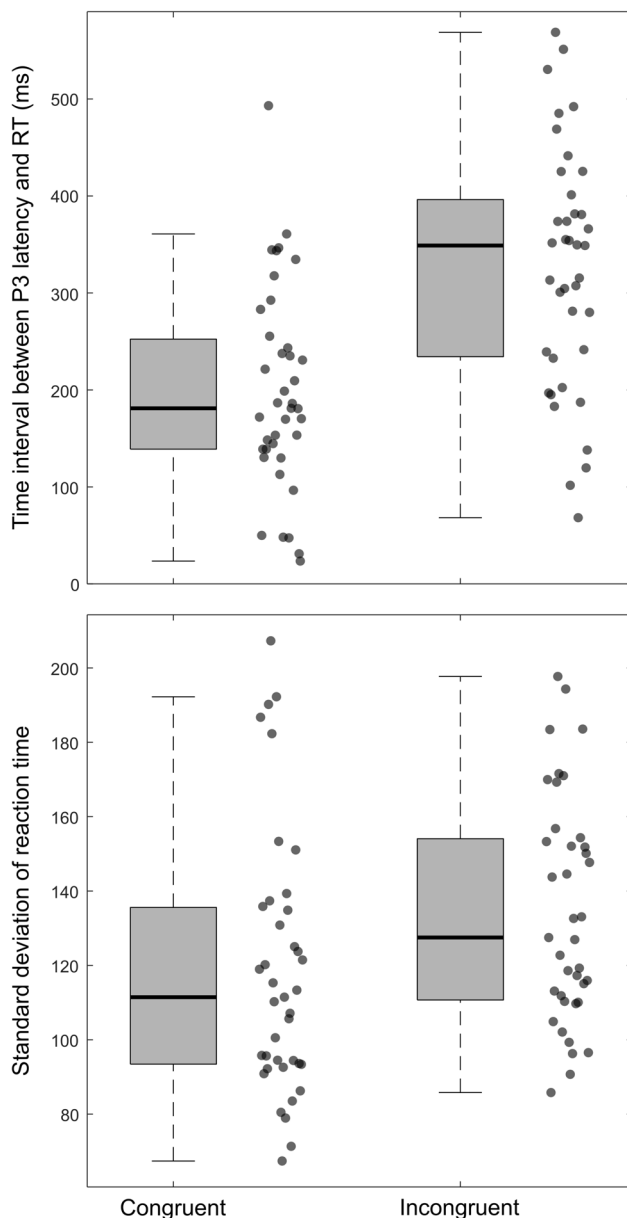
Fig. 6 The time interval between the reaction time and P3 latency in the Pz channel (top panel) and the standard deviation of reaction time (bottom panel), under the congruent and incongruent conditions. Both of these parameters were significantly higher in the incongruent condition

conditions led to synchronization of the theta band and desynchronization of the alpha band. Significant differences between these two conditions were observed in regard to the impact of the alerting network on the ERD/ERS. At the 300 ms after the target stimuli in the parietal-occipital region, there was significantly higher theta band synchronization observed in the no-cue condition compared to the double-cue condition. Also, significant differences were observed between the no-cue and double-cue conditions prior to the

appearance of the target stimuli, potentially due to the influence of the cue appearance.

The results of the event-related spectral perturbation analysis for the orienting network in the parietal and parieto-occipital regions are presented in Fig. 11. In the valid cue condition, which was consistent with the double-cue and no-cue conditions, theta band synchronization and alpha band desynchronization were observed. Notably, significant differences were observed between the valid cue and double-cue conditions in terms of the influence of the orienting network on the ERD/ERS patterns in the parietal and parietal-occipital regions. Specifically, in the parietal-occipital region, the synchronization of the theta band in the valid cue condition was significantly higher than that in the double-cue condition at 200 ms after the appearance of the target stimuli. Moreover, in the parietal region, the desynchronizations of the high beta and low gamma bands in the valid cue condition were significantly higher than those in at 600 ms after the target stimuli emerged.

Figure 12 presents the outcomes of the event-related spectral perturbation analysis conducted on the executive network observed in the Pz and Cz channels. Similar to the different cue conditions, the varying congruency conditions displayed synchronization of theta band activity and desynchronization of alpha band activity. Furthermore, the executive network demonstrated significant effects on patterns of ERD/ERS. Notably, significant synchronization of both the theta and alpha bands was observed in Cz, particularly between 450 and 750 ms following the presentation of the target stimuli.

EEG connectivity

Each connectivity matrix consisted of 32 rows and 32 columns, with each row or column corresponding to one EEG channel. The effect of the attentional network on brain connectivity was evaluated by comparing each pair of conditions associated with each network across subjects. Figure 13 shows significant changes in brain connectivity between two conditions corresponding to each network, measured in terms of correlation after applying multiple comparison corrections. Correlation changes between pairs of conditions related to the alerting and orienting networks appeared to be more transverse, while correlation changes between pairs of conditions related to the executive networks displayed a more longitudinal pattern. Correlation between channels with significant differences between the conditions related to each network was lower in the double-cue condition compared to the no-cue and valid cue conditions. Additionally, the incongruency of the target increased the correlation between the channels.

As seen in Fig. 14, the coherence between channels in the studied frequency bands had some significant differences
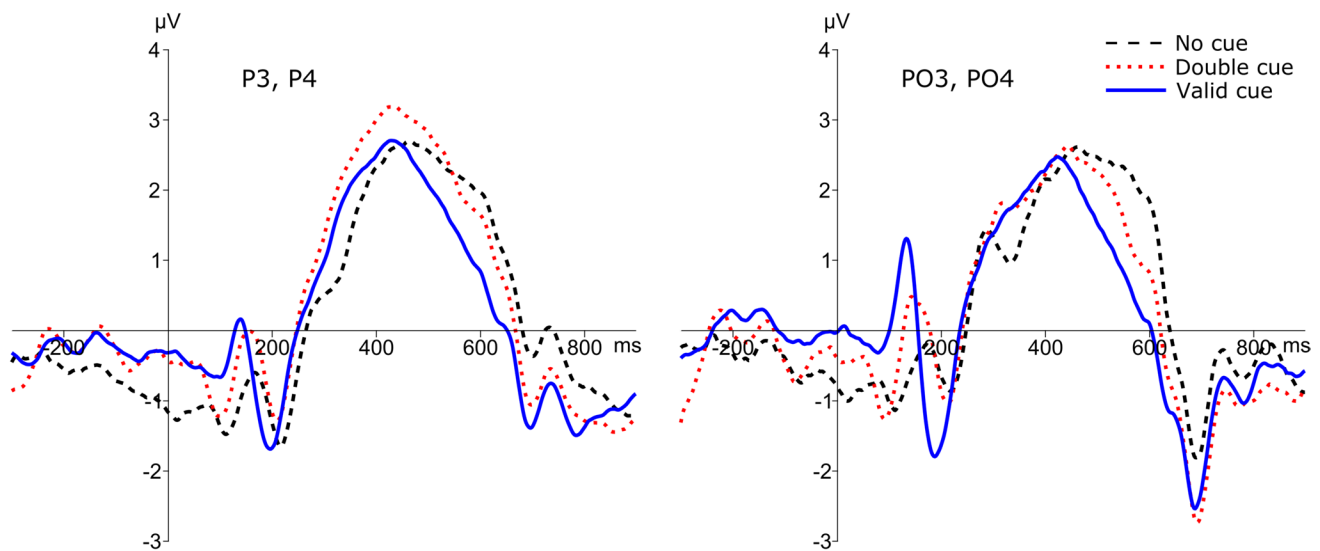
Fig. 7 Target-locked event-related potential (ERP) waveforms recorded in the parietal (left panel) and parieto-occipital (right panel) regions under different cue conditions. The ERPs are displayed for no cue (dash line), double cue (dot line), and valid cue (solid line) conditions. Significant differences were observed in the latency and amplitude of the P1 component in the parietal and parieto-occipital regions, respectively, as well as in the amplitude of the P1–N1 component in the parieto-occipital region, between the double-cue and no-cue conditions. Furthermore, significant differences were found in the latency of the P1 and N1 components in the parietal region, and in the amplitude of the P1, N1, and P1–N1 components in both the parietal and parieto-occipital regions, between the valid cue and double-cue conditions

Table 2 Amplitude (μV) and latency (ms) of target-locked P1 and N1 components by cue conditions and electrodes

		No cue Mean (SD)	Double cue Mean (SD)	Valid cue Mean (SD)	Alerting Mean (SD)	Orienting Mean (SD)	Alerting p (Cohen's d)	Orienting p (Cohen's d)
P1 in P3, P4	Amplitude	− 0.7 (1.93)	− 0.09 (1.4)	− 0.04 (1.39)	− 0.61 (1.98)	− 0.05 (1.42)	> 0.05 (− 0.36)	> 0.05 (− 0.036)
	Latency	162 (23)	155 (17)	143 (16)	6 (16)	13 (16)	0.02 (0.31)	< 0.001 (0.72)
N1 in P3, P4	Amplitude	− 1.46 (1.66)	− 1.09 (1.32)	− 1.54 (1.47)	− 0.36 (2.16)	0.44 (1.73)	> 0.05 (− 0.24)	> 0.05 (0.32)
	Latency	211 (23)	206 (22)	198 (17)	5 (27)	9 (18)	> 0.05 (0.21)	0.006 (0.44)
P1 in PO3, PO4	Amplitude	− 0.29 (1.9)	0.33 (2.11)	0.95 (1.77)	− 0.62 (1.59)	− 0.62 (1.57)	0.02 (− 0.31)	0.017 (− 0.32)
	Latency	157 (27)	150 (9)	138 (16)	6 (25)	12 (19)	> 0.05 (0.28)	< 0.001 (0.68)
N1 in PO3, PO4	Amplitude	− 0.74 (2.2)	− 0.85 (1.97)	− 1.6 (1.71)	0.1 (1.6)	0.76 (1.78)	> 0.05 (0.05)	0.011 (0.4)
	Latency	201 (31)	204 (24)	191 (23.13)	− 3 (36.23)	13 (21)	> 0.05 (− 0.1)	< 0.001 (0.54)
(P1–N1) in P3, P4	Amplitude	0.76 (1.5)	1 (1.42)	1.5 (1.44)	− 0.24 (1.04)	− 0.49 (1.29)	> 0.05 (− 0.17)	0.022 (− 0.34)
	Latency	− 49 (27)	− 51 (20)	− 55 (18)	2 (34)	4 (23)	> 0.05 (0.07)	> 0.05 (0.21)
(P1–N1) in PO3, PO4	Amplitude	0.45 (2.25)	1.17 (2.15)	2.56 (2.47)	− 0.72 (1.8)	− 1.38 (2.2)	0.017 (− 0.33)	< 0.001 (− 0.58)
	Latency	− 44 (39)	− 53 (24)	− 53 (28)	9 (46)	− 1 (28)	> 0.05 (0.28)	> 0.05 (− 0.02)

SD standard deviation

between the conditions corresponding to the alerting and orienting networks after multiple comparison corrections. Partly, the same transverse patterns observed in the correlation for these networks were also observed in coherence, especially in the theta band. Overall, in the theta band, the coherence of the double-cue condition was higher than the no-cue and valid cue conditions, and it was the opposite in the alpha and beta bands. For the executive network, the coherence in the theta and alpha bands had significant differences between congruent and incongruent conditions in a lot of channels. The pattern of coherence changes between different conditions of congruency in the theta band was mainly longitudinal, and in
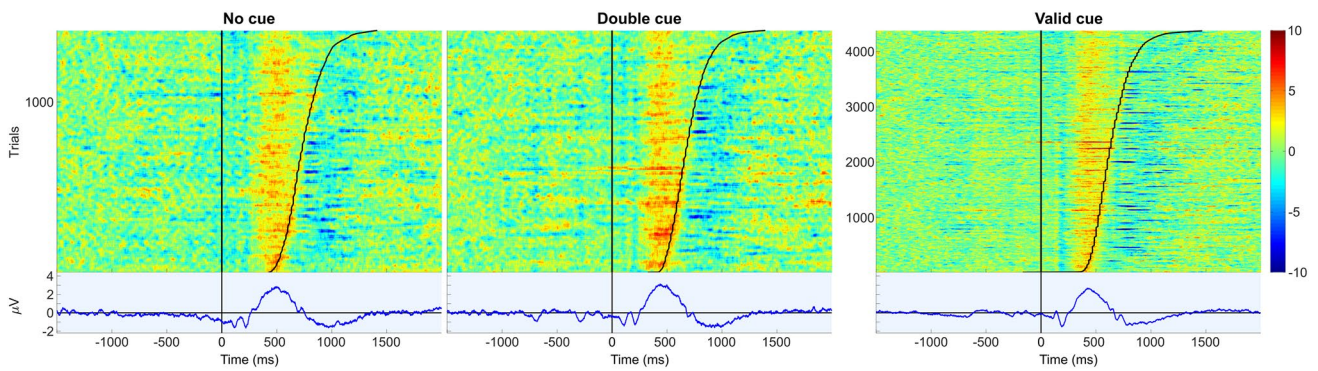
Fig. 8 The ERP images sorted based on the reaction time in the no-cue, double-cue, and valid cue conditions in the P3 channel
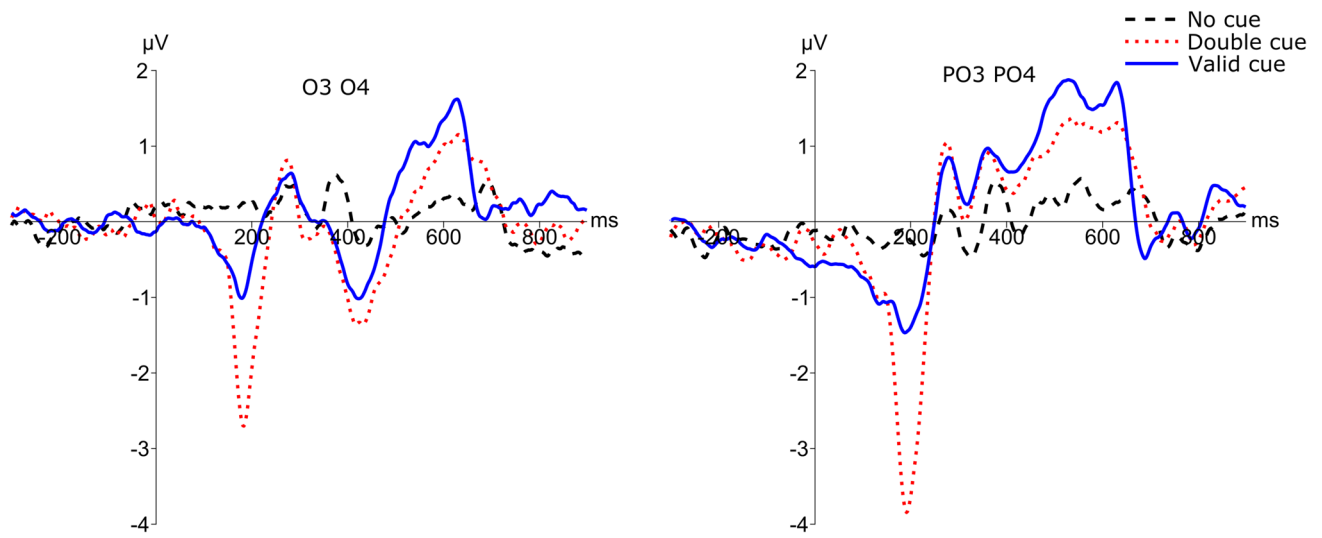

Fig. 9 Cue-locked ERP waveforms along occipital (left panel) and parieto-occipital (right panel) regions under different cue conditions. The ERPs are depicted for the no-cue (dash line), double-cue (dot line), and valid cue (solid line) conditions. Notably, significant differences in N1 amplitudes were observed among all three cue conditions in both the occipital and parieto-occipital regions

Table 3 Cue-locked N1 amplitude (μV) across different cue conditions and electrodes

	No cue Mean (SD)	Valid cue Mean (SD)	Double cue Mean (SD)	Valid–no cue p-value (Cohen's d)	Double–valid cue p-value (Cohen's d)
O1, O2	− 0.72 (0.75)	− 1.64 (1.21)	− 3.53 (2.19)	< 0.001 (− 0.84)	< 0.001 (− 0.95)
PO3, PO4	− 1.22 (0.79)	− 2.19 (1.44)	− 4.66 (2.2)	0.002 (− 0.77)	< 0.001 (-1.11)

SD standard deviation

the alpha band, in addition to longitudinal patterns, transverse patterns were observed, especially in the frontal region. Also, the coherence in the beta band significantly differed between the congruent and incongruent conditions in the parietal region, and its pattern was transverse. Unlike the correlation

Table 4 Correlation coefficients and significance levels between alerting network score, amplitude, and latency of target-locked P1 and N1 by cue conditions associated with the alerting network

		Double cue r (p-value)	No cue r (p-value)	Double–no cue r (p-value)
P1 in P3, P4	Amplitude	0.2 (>0.05)	− 0.07 (>0.05)	0.2 (>0.05)
	Latency	− 0.12 (>0.05)	0.03 (>0.05)	− 0.17 (>0.05)
N1 in P3, P4	Amplitude	− 0.07 (>0.05)	− 0.3 (>0.05)	0.19 (>0.05)
	Latency	0.04 (>0.05)	0.13 (>0.05)	− 0.08 (>0.05)
P1 in PO3, PO4	Amplitude	− 0.08 (>0.05)	− 0.1 (>0.05)	0.02 (>0.05)
	Latency	− 0.1 (>0.05)	0.13 (>0.05)	− 0.22 (>0.05)
N1 in PO3, PO4	Amplitude	− 0.4 (0.012)	− 0.32 (0.049)	− 0.06 (>0.05)
	Latency	0.25 (>0.05)	0.02 (>0.05)	0.14 (>0.05)
(P1–N1) in P3, P4	Amplitude	0.26 (>0.05)	0.25 (>0.05)	0 (>0.05)
	Latency	− 0.14 (>0.05)	− 0.08 (>0.05)	− 0.02 (0>0.05)
(P1–N1) in PO3, PO4	Amplitude	0.29 (>0.05)	0.22 (>0.05)	0.07 (>0.05)
	Latency	− 0.33 (0.041)	0.07 (>0.05)	− 0.23 (>0.05)

Table 5 Correlation coefficients and significance levels between orienting network score, amplitude, and latency of target-locked P1 and N1 by cue conditions associated with the orienting network

		Valid cue r (p-value)	Double cue r (p-value)	Valid–double cue r (p-value)
P1 in P3, P4	Amplitude	0.15 (>0.05)	− 0.03 (>0.05)	0.17 (>0.05)
	Latency	− 0.04 (>0.05)	− 0.1 (>0.05)	0.07 (>0.05)
N1 in P3, P4	Amplitude	0.09 (>0.05)	0.2 (>0.05)	− 0.07 (>0.05)
	Latency	− 0.16 (>0.05)	0.07 (>0.05)	− 0.24 (>0.05)
P1 in PO3, PO4	Amplitude	0.12 (>0.05)	0.16 (>0.05)	− 0.08 (>0.05)
	Latency	− 0.09 (>0.05)	− 0.15 (>0.05)	0.08 (>0.05)
N1 in PO3, PO4	Amplitude	0.01 (>0.05)	0.42 (0.008)	− 0.45 (0.004)
	Latency	− 0.18 (>0.05)	− 0.23 (>0.05)	0.06 (>0.05)
(P1–N1) in P3, P4	Amplitude	0.05 (>0.05)	− 0.21 (>0.05)	0.28 (>0.05)
	Latency	0.12 (>0.05)	− 0.16 (>0.05)	0.24 (>0.05)
(P1–N1) in PO3, PO4	Amplitude	0.08 (>0.05)	− 0.23 (>0.05)	0.31 (>0.05)
	Latency	0.1 (>0.05)	0.11 (>0.05)	0 (>0.05)

between channels, which was higher in the incongruent condition than in the congruent condition, the coherence in all three frequency bands was lower in the incongruent condition than that in the congruent condition.

Discussion

This study aimed to examine different conditions related to attention networks on various aspects of brain electrophysiological dynamics, including event-related potentials, event-related spectral perturbation, and brain connectivity. Additionally, the study explored the relationship between scores and ERP components.

According to Figs. 3 and 4 and Table 1, the P3 analysis revealed a significant topographical difference between the different conditions of the target. Specifically, in the parietal region, the P3 amplitude was found to be significantly lower in the incongruent condition compared to the congruent condition (p-value = 0.002). Additionally, central area, the mean amplitude in the time interval of 350–700 ms for target-locked P3 was significantly lower in the incongruent condition compared to the congruent condition (p-value = 0.0144). These findings are consistent studies that have also reduction in the P3 component in the central and parietal regions (Gonçalves et al. 2018; He et al. 2021; Hershaw et al. 2020; Kałamała et al. 2018; Kaufman et al. 2016; Neuhaus et al. 2010). This decrease in the P3 amplitude has been attributed to the inhibition effect, indicating that tasks with high cognitive load limit attention resources, leading to a reduction in P3 amplitude (Polich 2007). Research findings indicate that older adults, compared to younger adults, have a more pronounced decrease in P3 amplitude in the incongruent condition (Kaufman et al. 2016), which may be attributed to the increased task difficulty for older subjects. Despite the observed decrease in P3 amplitude in the incongruent condition in the parietal and central regions, there was no
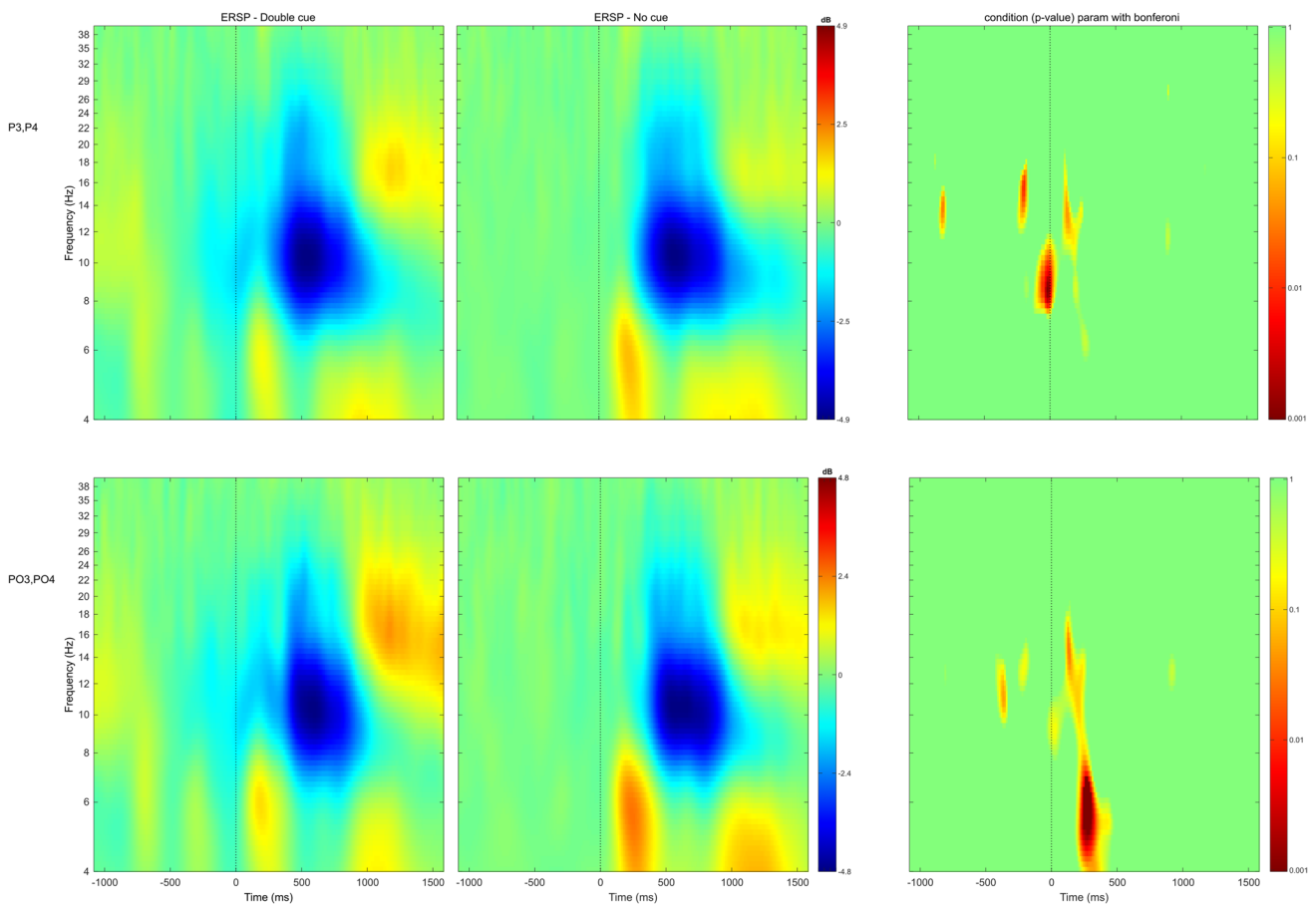
Fig. 10 Event-related spectral perturbation comparing the double-cue (left) and no-cue (middle) conditions in the parietal (top) and parieto-occipital (bottom) regions. The right panels display *p*-values, adjusted for multiple comparisons using the Bonferroni correction, indicating significance between the two conditions

significant difference between these two conditions considering the area under the curve in proportion to the distance between the two zero-crossing points of this component. Moreover, in this study and other studies (Kałamała et al. 2018; Ma et al. 2020; Neuhaus et al. 2010; Williams et al. 2016; Xue et al. 2022; Yang and Xiang 2019; D. Zhang et al. 2018), visually, it has been observed that the P3 component in the parietal and central regions exhibited a broader width and a longer decline in the incongruent condition compared to the congruent condition. Considering this issue, it is possible to propose the hypothesis that the brain's response to incongruent stimuli may have more variability and temporal diversion than to the congruent stimuli, and at the single trial level, this level of difference between congruent and incongruent conditions may not exist.

Especially, according to Fig. 5, in the incongruent condition, compared to the congruent condition, there is more variation in the interval between reaction times and the P3 component at the single trial level. The greater distance of the response time from the P3 component can reduce the

synergistic effect of the response-related potentials on the P3 component. Additionally, as shown in Fig. 12, theta band synchronization takes more time following the incongruent targets compared to the congruent targets in the Cz channel. This pattern is similar to the inhibition effect observed in the right cingulate gyrus reported in another study (Chikara and Ko 2019). The theta power is sensitive to the utilization of executive control in congruency conditions (Nigbur et al. 2011). According to (Wang and Ding 2011), the theta synchronization may largely result from trial-to-trial variations of the P3 in both amplitude and latency. On the other hand, the fact that theta synchronization takes longer can cause ERP components to expand. Besides theta synchronization, there was a significant increase in alpha desynchronization in the incongruent condition. These findings support studies that link theta ERS and alpha ERD to executive or inhibition processes (Janssens et al. 2018; Klimesch et al. 2007; McDermott et al. 2017).

In a limited number of studies, the impact of alerting and orienting networks on ERP components has not been
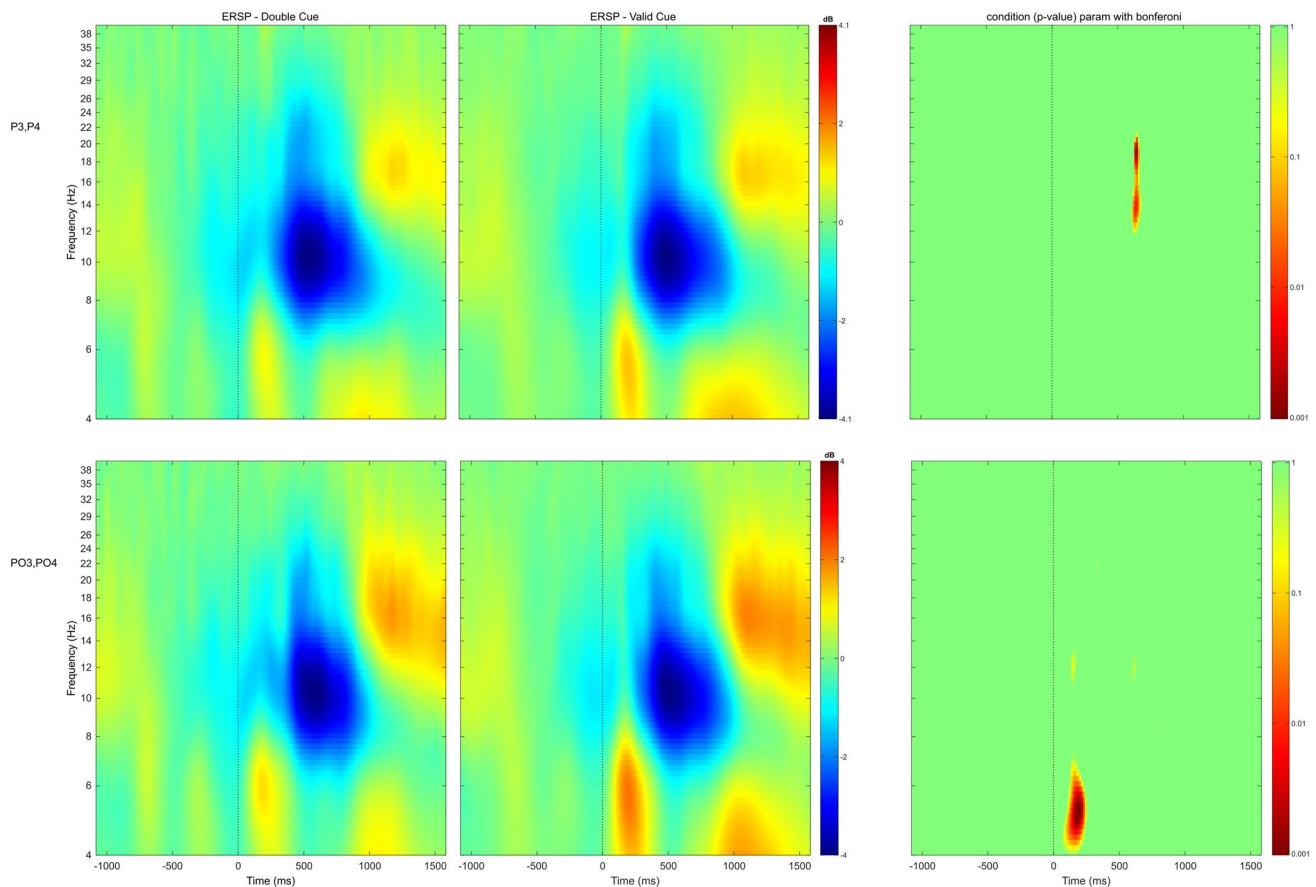
Fig. 11 Event-related spectral perturbation for the double-cue (left) and valid cue (middle) conditions in the parietal (top) and parieto-occipital (bottom) regions. The right panels display *p*-values after the Bonferroni correction comparing the two conditions

observed. For instance, Vázquez-Marrufo et al. found no significant effects of the alerting and orienting networks in the parieto-occipital region for the (target-locked) P1 and N1 components. (Vázquez-Marrufo et al. 2014). However, in the present study, as indicated in Table 2, some effects of these networks were discovered in the parietal and parieto-occipital regions.

The target-locked P1 latency in the parietal region was found to be greater in the no-cue condition compared to the double-cue condition. Additionally, the P1 latency was higher in the double-cue condition compared to the valid spatial cue condition. These findings indicate the presence of alerting and orienting effects, with small and large effect sizes, respectively, in the parietal region. Moreover, a significant orienting effect in P1 latency was observed in the parieto-occipital region, again with a large effect size. The faster initiation of attention-related processes at the sensory level may account for part of the improvement in behavioral performance. Notably, such effects were not found in a previous study conducted in the parieto-occipital region (Galvao-Carmona et al. 2014). Although only a few studies have statistically examined the impact of attentional networks on

P1 latency, in some studies, such as (Santhana Gopalan et al. 2019), the effect of alerting and orienting networks on the latency of P1 is observable visually. Thus, further research is warranted to investigate the effect of attention networks on P1 latency.

Target-locked P1 amplitude and P1-N1 amplitude in the parieto-occipital region were higher in the valid spatial cue condition compared to the double cue condition and higher in the double-cue condition compared to the no cue condition. Therefore, significant alerting and orienting effects were observed in the parietal region with small effect sizes and in the parieto-occipital region with small and medium effect sizes, respectively. Additionally, a significant orienting effect was observed in P1-N1 amplitude with a small effect size in the parietal region. These findings indicate that knowing the time and location of the target stimuli enhances the P1 amplitude. This aligns with previous studies that associated higher P1 amplitude with stimuli presented at the attended location (Clark and Hillyard 1996; Hillyard et al. 1998; Posner and Dehaene 1994). Racer et al., similar to our study, reported significant effects of alerting and orienting on the P1 amplitude were larger in the central cue condition
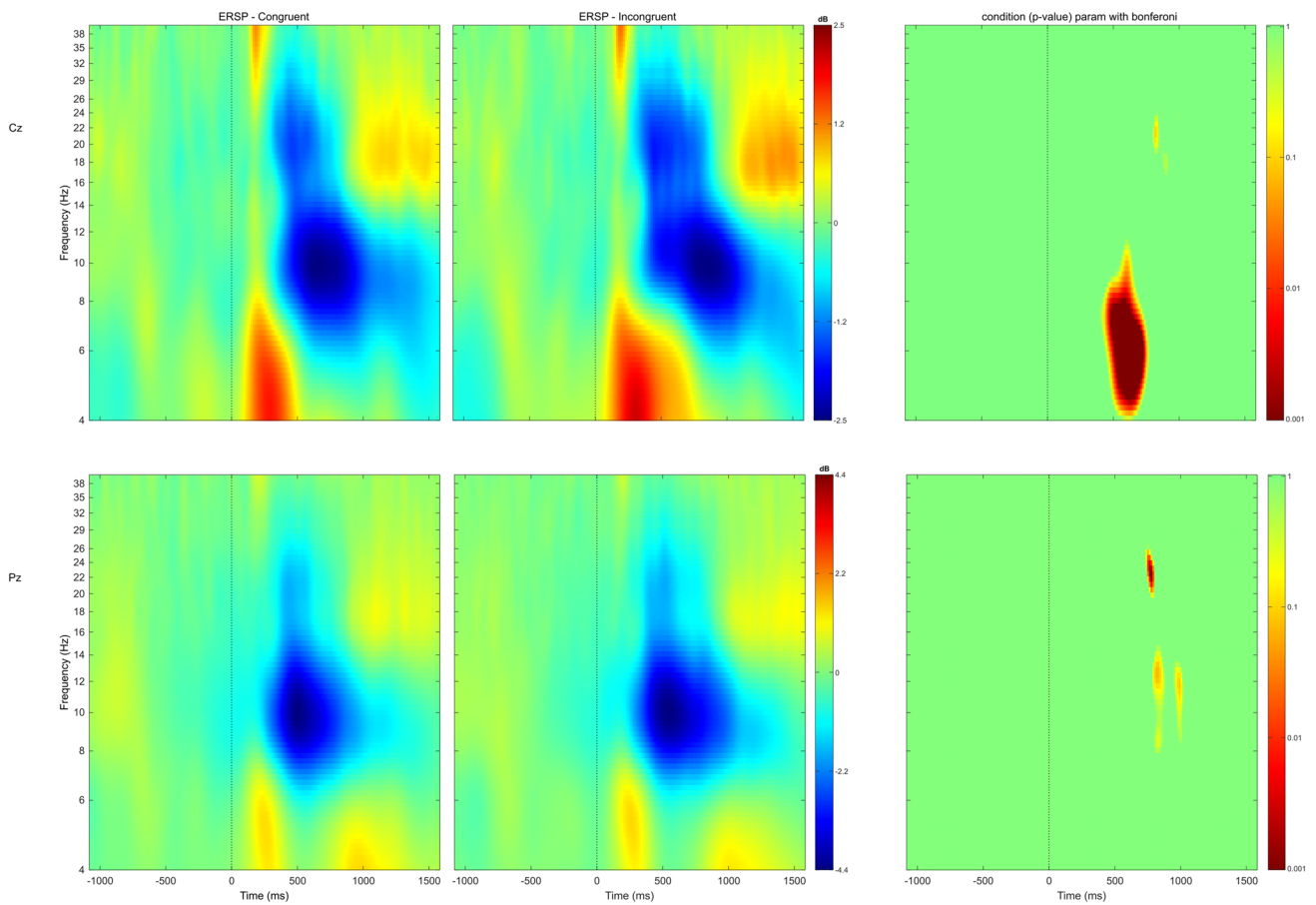
Fig. 12 Event-related spectral perturbation for congruent (left) and incongruent (middle) conditions at the Cz (top) and Pz (bottom) channel locations. The right panels display the *p*-values after the Bonferroni correction between the two conditions
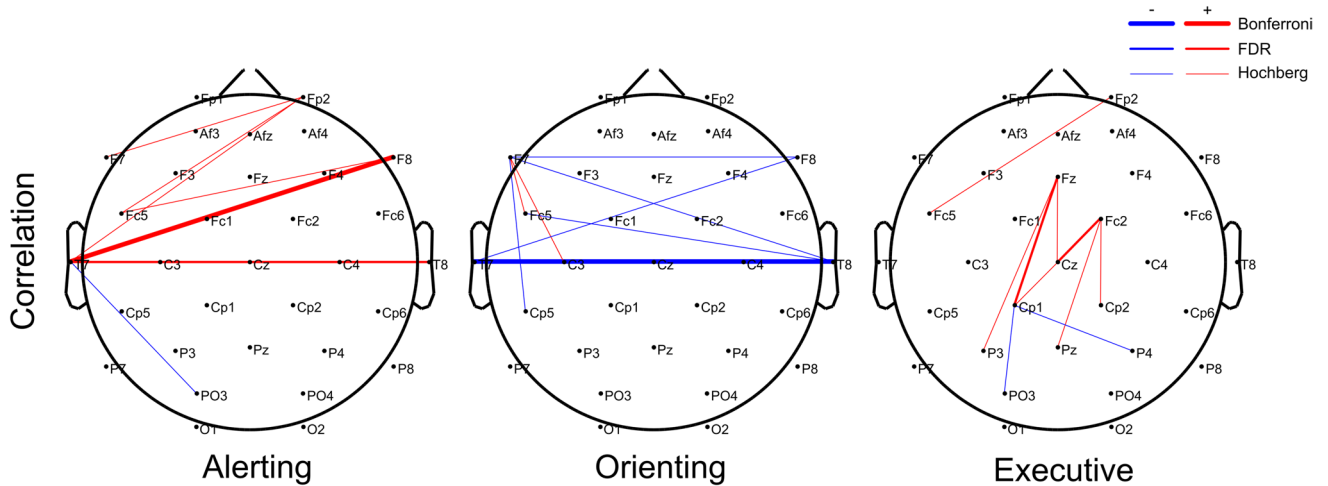

Fig. 13 Significant changes in the channels correlation between the conditions corresponding to each attention network. The method of subtraction of correlation between conditions is the same as how to calculate the score of each network
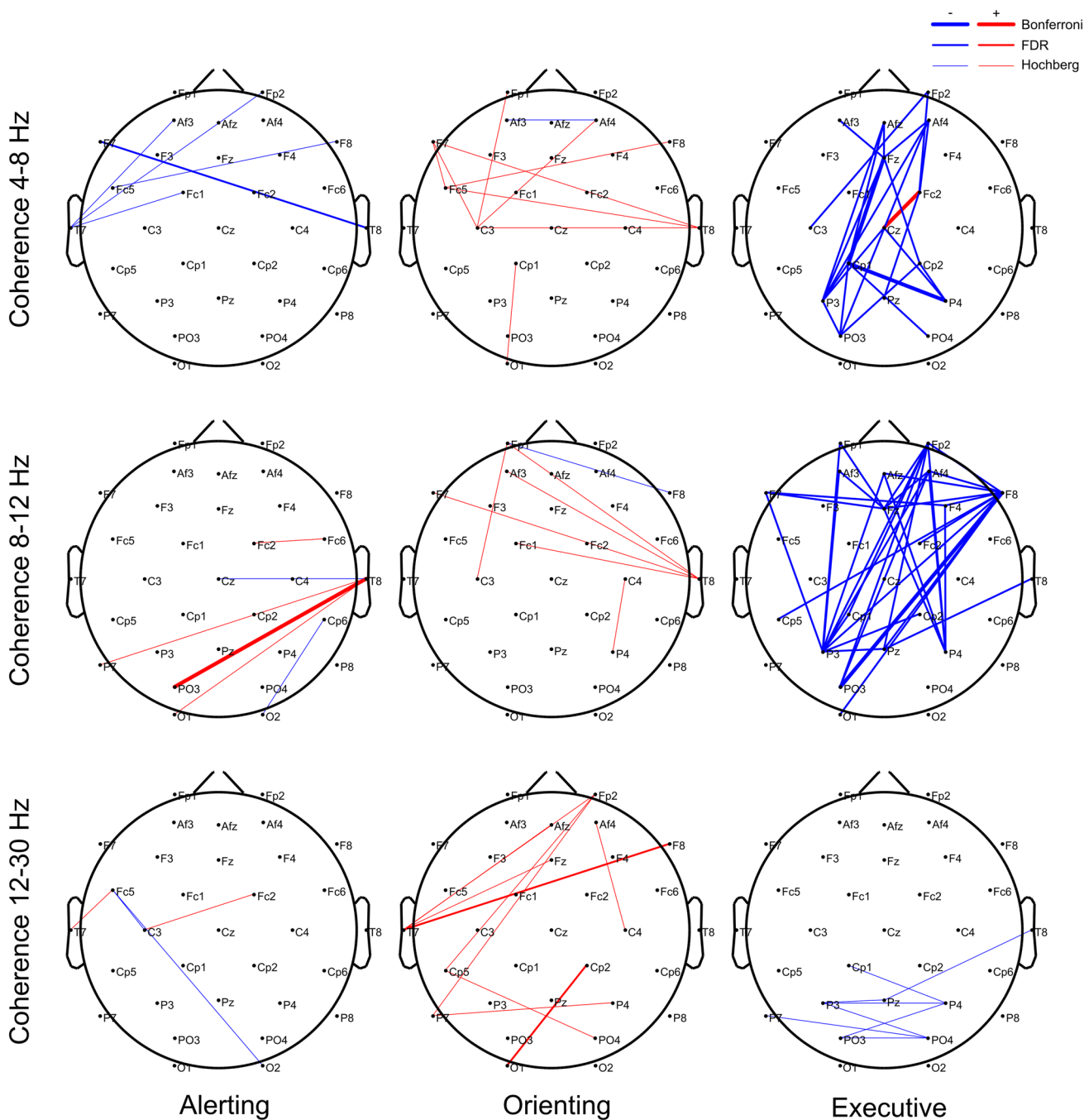
Fig. 14 Significant changes in the coherence of channels within three frequency bands corresponding to each attention network condition. The method used to subtract coherence between conditions is consistent with the calculation of the score for each network

compared to the no-cue condition and larger in the spatial cue condition compared to the central cue condition (Racer et al. 2011). Additionally, in the Galvao-Carmona study, a significant orienting effect was observed on the target-locked P1 amplitude with the spatial cue condition showing larger amplitudes compared to the central cue condition. The authors suggested that the larger P1 amplitudes may be a contributing factor to the improvement in behavioral

performance (Galvao-Carmona et al. 2014). Gonçalves et al. reported a significant alerting effect in the target-locked P1 amplitude, but in the opposite direction of our present study, the P1 amplitude was larger in the no-cue condition compared to the double-cue condition (Gonçalves et al. 2018). Also, Williams et al., like Gonçalves et al., reported a significant alerting effect in the target-locked P1 amplitude again in the opposite direction of our current study (Williams

et al. 2016). The discrepancy between these two studies and our present study may be attributed to the selection of an inappropriate period for baseline removal. In the studies of Gonçalves et al. and Williams et al., epochs were baseline-corrected according to 100 ms and 200 ms before the target, respectively, while the interval between the cue and the target was 400 ms in both studies (Gonçalves et al. 2018; Williams et al. 2016). In the no-cue condition, no evoked potential is expected before the target. However, in the double-cue condition of these two studies, due to the short time interval between the cue and the target, it is possible that the effects of cue-dependent evoked potentials existed in the time interval before the target (which was considered for baseline removal of epochs). This presence of evoked effects before the targets preceded by a double cue may have led to an incorrect baseline removal process of epochs. Additionally, upon visual inspection of the ERP waveforms in these two studies, it is evident that the target-locked ERP waveforms for the no-cue condition generally exhibit higher amplitude compared to the double-cue condition (this is not limited to the P1 amplitude). This observation also raises concerns regarding the accuracy of the baseline removal process. Concerning the studies that support the findings of the present study regarding P1 amplitude, it is noted that in the studies conducted by Racer et al. and Galvao-Carmona et al., the cue-to-target interval was 1000 ms. This interval was likely sufficiently long to eliminate the evoked effects by the cues. Furthermore, visually, there appears to be no considerable vertical shift observed between the ERP waveforms associated with different cue conditions (Galvao-Carmona et al. 2014; Racer et al. 2011). In our present study, the interval between the cue and the target was variable (0, 400, and 800 ms). However, the selected time interval to remove the baseline of epochs was before the presentation of the cues (1500 to 900 ms before the target).

The target-locked N1 latency in the parieto-occipital and parietal regions was significantly greater in the double-cue condition compared to the valid spatial cue condition, indicating a significant orienting effect in the N1 latency. It is worth noting that none of the networks examined showed a significant impact on the latency difference between the P1 and N1 peaks, indicating that the faster N1 peak may be attributed to the quicker initiation of activities rather than faster processes leading up to this stage. Furthermore, the impact of attentional networks on target-locked N1 latency remains poorly investigated. However, several studies have visually demonstrated the impact of alerting or orienting networks on the latency of this component (Neuhaus et al. 2010; Santhana Gopalan et al. 2019; Yang and Xiang 2019). Additional research is likely necessary to thoroughly evaluate the influence of attentional networks on N1 latency.

The target-locked N1 amplitude in the parieto-occipital region and the difference in P1 and N1 amplitudes in the parietal region exhibited a significant orienting effect. Furthermore, the difference in P1 and N1 amplitudes in the parieto-occipital region demonstrated both alerting and orienting effects, significantly. This finding aligns with a majority of studies that have reported significant effects for alerting or orienting networks, where the N1 amplitude was found to be higher in cue conditions associated with faster reaction times. Specifically, the N1 amplitude was greater in the temporal cue condition compared to the no-cue condition, and it was higher in the spatial cue condition compared to the temporal cue condition, as observed in the present study (Gonçalves et al. 2018; Kalia et al. 2018; Kaufman et al. 2016; Neuhaus et al. 2010; Santhana Gopalan et al. 2019; Williams et al. 2016; Zhang et al. 2021). Higher N1 peak amplitude may potentially contribute to faster reaction times at the behavioral level.

According to Figs. 10 and 11, target-locked theta synchronization was significantly lower in the double-cue condition compared to the no-cue and valid cue conditions in the parieto-occipital region. It is worth noting that theta synchronization is known to be positively correlated with the ability to encode new information (Klimesch 1999). The observed higher theta synchronization in the no-cue condition, compared to the double-cue condition, can be attributed to the higher presence of new information in the no-cue condition. However, this explanation does not hold for the fact that theta synchronization is higher in the valid cue condition than in the double-cue condition. This discrepancy can possibly be explained by the substantial differences observed in the period before the target stimulation, which is utilized as the baseline period for relative power estimation in the analysis, between the two conditions.

According to Fig. 9 and Table 3, the cue-locked N1 amplitude was found to be higher in the occipital and parieto-occipital areas in the double-cue condition compared to both the single-cue condition and the no-cue condition. Similarly, the single-cue condition exhibited higher N1 amplitude compared to the no-cue condition. These results were anticipated considering the varying degrees of visual stimulation across the cue conditions, and they likely do not stem from attentional network effects, in contrast to some prior research. The observation of cue-locked N1 amplitude differences across various cue conditions has been reported in other studies (Williams et al. 2016; Yang and Xiang 2019).

Based on the findings presented in Table 4, the alerting network score exhibited a significant correlation with the N1 amplitude in the parieto-occipital region under both the no-cue and double-cue conditions. Additionally, a significant correlation was observed between the alerting network score and the time interval between the P1 and N1 peaks in the double-cue condition. These results indicate that subjects with higher N1 peak amplitudes in the parieto-occipital region under both cue conditions have higher alerting scores. Additionally,

subjects with shorter time intervals between the N1 and P1 peaks in the double-cue condition also exhibited higher alerting scores. Based on Table 5, there are significant correlations between the amplitude of N1 in the parieto-occipital region in the double-cue condition and the difference in N1 amplitude between the spatial valid cue condition and the double-cue condition, with the orienting score. This suggests that subjects with higher N1 amplitude in the double-cue condition in this region tend to have a lower orienting score. On the other hand, subjects with a higher difference in N1 amplitude between the double-cue and the valid cue conditions tend to have a higher orienting score. It is worth noting that, in addition to the effects of attention networks on ERP components, the efficiencies of the alerting and orienting networks also exhibit significant correlations with ERP components. According to the evidence from the present study, the N1 amplitude in different cue conditions displayed significant correlations with the efficiency of alerting and orienting networks. Therefore, it may be possible to utilize the ERP components, in conjunction with reaction time, to assess the score of attention networks in both normal and patient subjects.

Disregarding the Hochberg multiple comparisons correction method, significant differences were observed only in the coherence of theta and alpha bands, specifically about the executive network conditions. The coherence within these bands notably decreased in the incongruent condition compared to the congruent condition. This observation may be attributed to the higher workload associated with the incongruent condition, which results in limited resources available for communication across different parts.

One of the limitations of this study is that all the samples consisted of a singular gender. This restricts the generalizability of the results to encompass all genders. Additionally, conducting more trials in each condition would have been advantageous in obtaining more reliable results, particularly in correlational analyses of the scores of networks with ERP components. This issue should be taken into account in future studies. Further, it is possible that the application of baseline correction with a long time interval preceding the target stimulus could have rendered the waveform somewhat unreliable. Nonetheless, it was decided to utilize the pre-cue time intervals for baseline correction due to the potential presence of cue-dependent potentials near the target stimulation.

In this study, distinct topographic features of brain electrical activity were observed for each combination of the two conditions used to calculate the efficiency of each network. Furthermore, significant correlations were found between the score of attention networks and certain ERP components. However, the relationship between attention networks and brain electrophysiological activity has produced inconsistent results across various studies. Therefore, further research in this area is necessary. Additionally, the temporal variation of reaction times in the incongruent condition was found to be greater than that in the congruent condition. Moreover, the time interval between the response time and the P3 component showed more variation in the incongruent condition. Therefore, in addition to factors such as the inhibition effect or task difficulty contributing to the lower amplitude of the P3 component in the incongruent condition, consideration should also be given to asynchrony at the single trial or single subject levels. Also, based on our survey, no study has been conducted regarding the relationship between ERP components and the efficiency of attention networks. Therefore, we recommend conducting further studies to explore the connection between attention network efficiency and brain electrical activity. The present study serves as a significant milestone in conducting future research on the use of ERP components to evaluate attention network efficiency, as well as investigating the impact of various diseases and conditions on ERP components related to attention networks. Furthermore, the results of this study can contribute to the investigation of the effect of various diseases on other electrophysiological features of the brain, such as connectivity and ERD/ERS, which are associated with attention networks. Future studies can also explore the outcome of rehabilitation interventions on these features in different ways.

Declarations

Conflict of interest The authors declare that they have no conflict of interest.

References

Bigdely-Shamlo N, Mullen T, Kothe C, Su K-M, Robbins KA (2015) The PREP pipeline: standardized preprocessing for large-scale EEG analysis. Front Neuroinform 9:16

Chikara RK, Ko L-W (2019) Modulation of the visual to auditory human inhibitory brain network: an EEG dipole source localization study. Brain Sci 9(9):216

Clark VP, Hillyard SA (1996) Spatial selective attention affects early extrastriate but not striate components of the visual evoked potential. J Cogn Neurosci 8(5):387–402

Delorme A, Makeig S (2004) EEGLAB: an open source toolbox for analysis of single-trial EEG dynamics including independent component analysis. J Neurosci Methods 134(1):9–21

Eriksen BA, Eriksen CW (1974) Effects of noise letters upon the identification of a target letter in a nonsearch task. P&P 16(1):143–149

Fan J, Gu X, Guise KG, Liu X, Fossella J, Wang H, Posner MI (2009) Testing the behavioral interaction and integration of attentional networks. Brain Cogn 70(2):209–220. https://doi.org/10.1016/j.bandc.2009.02.002

Fan J, McCandliss BD, Sommer T, Raz A, Posner MI (2002) Testing the efficiency and independence of attentional networks. J Cogn Neurosci 14(3):340–347. https://doi.org/10.1162/089892902317361886

Galvao-Carmona A, González-Rosa J, Hidalgo-Muñoz A, Páramo D, Benítez M, Izquierdo G, Vázquez-Marrufo M (2014) Disentangling the attention network test: behavioral, event related potentials, and neural source analyses. Front Hum Neurosci 8:813

Gonçalves ÓF, Rêgo G, Conde T, Leite J, Carvalho S, Lapenta OM, Boggio PS (2018) Mind wandering and task-focused attention: ERP correlates. Sci Rep 8(1):7608. https://doi.org/10.1038/s41598-018-26028-w

He C, Chikara RK, Yeh C-L, Ko L-W (2021) Neural dynamics of target detection via wireless EEG in embodied cognition. Sensors 21(15):5213

Hershaw J, Hill-Pearson CA, Arango JI, Souvignier AR, Pazdan RM (2020) Changes in attentional processing following neurofeedback in patients with persistent post-concussive symptoms: a pilot study. Brain Inj 34(13–14):1723–1731

Hillyard SA, Vogel EK, Luck SJ (1998) Sensory gain control (amplification) as a mechanism of selective attention: electrophysiological and neuroimaging evidence. Philos Trans R Soc Lond B Biol Sci 353(1373):1257–1270

Janssens C, De Loof E, Boehler CN, Pourtois G, Verguts T (2018) Occipital alpha power reveals fast attentional inhibition of incongruent distractors. Psychophysiology 55(3):e13011. https://doi.org/10.1111/psyp.13011

Kałamała P, Drożdżowicz A, Szewczyk J, Marzecová A, Wodniecka Z (2018) Task strategy may contribute to performance differences between monolinguals and bilinguals in cognitive control tasks: ERP evidence. J Neurolinguistics 46:78–92

Kalia V, Thomas R, Osowski K, Drew A (2018) Staying alert? Neural correlates of the association between grit and attention networks. Front Psychol 9:1377

Kaufman DA, Sozda CN, Dotson VM, Perlstein WM (2016) An event-related potential investigation of the effects of age on alerting, orienting, and executive function. Front Aging Neurosci 8:99

Kleiner M, Brainard D, Pelli D (2007) What's new in Psychtoolbox-3?

Klimesch W (1999) EEG alpha and theta oscillations reflect cognitive and memory performance: a review and analysis. Brain Res Rev 29(2):169–195. https://doi.org/10.1016/S0165-0173(98)00056-3

Klimesch W, Sauseng P, Hanslmayr S (2007) EEG alpha oscillations: the inhibition–timing hypothesis. Brain Res Rev 53(1):63–88. https://doi.org/10.1016/j.brainresrev.2006.06.003

Lopez-Calderon J, Luck SJ (2014) ERPLAB: an open-source toolbox for the analysis of event-related potentials. Front Hum Neurosci 8:213

Ma H, Zhang X, Wang Y, Ma H, Cheng Y, Zhang F, Zhang D (2020) Overactive alerting attention function in immigrants to high-altitude Tibet

McDermott TJ, Wiesman AI, Proskovec AL, Heinrichs-Graham E, Wilson TW (2017) Spatiotemporal oscillatory dynamics of visual selective attention during a flanker task. Neuroimage 156:277–285. https://doi.org/10.1016/j.neuroimage.2017.05.014

Menyhart O, Weltz B, Győrffy B (2021) MultipleTesting.com: a tool for life science researchers for multiple hypothesis testing correction. PloS One 16(6):e0245824

Neuhaus AH, Hahn E, Hahn C, Ta TMT, Opgen-Rhein C, Urbanek C, Dettling M (2011) Visual P3 amplitude modulation deficit in schizophrenia is independent of duration of illness. Schizophr Res 130(1–3):210–215

Neuhaus AH, Urbanek C, Opgen-Rhein C, Hahn E, Ta TMT, Koehler S, Dettling M (2010) Event-related potentials associated with attention network test. Int J Psychophysiol 76(2):72–79

Nigbur R, Ivanova G, Stürmer B (2011) Theta power as a marker for cognitive interference. Clin Neurophysiol 122(11):2185–2194. https://doi.org/10.1016/j.clinph.2011.03.030

Oostenveld R, Fries P, Maris E, Schoffelen J-M (2011) FieldTrip: open source software for advanced analysis of MEG, EEG, and invasive electrophysiological data. Comput Intell Neurosci 2011:1–9

Pion-Tonachini L, Kreutz-Delgado K, Makeig S (2019) ICLabel: an automated electroencephalographic independent component classifier, dataset, and website. Neuroimage 198:181–197

Polich J (2007) Updating P300: an integrative theory of P3a and P3b. Clin Neurophysiol 118(10):2128–2148

Posner MI (1980) Orienting of attention. Q J Exp Psychol 32(1):3–25

Posner MI, Dehaene S (1994) Attentional networks. Trends Neurosci 17(2):75–79

Racer KH, Gilbert TT, Luu P, Felver-Gant J, Abdullaev Y, Dishion TJ (2011) Attention network performance and psychopathic symptoms in early adolescence: An ERP study. J Abnorm Child Psychol 39(7):1001–1012

Santhana Gopalan PR, Loberg O, Hämäläinen JA, Leppänen PH (2019) Attentional processes in typically developing children as revealed using brain event-related potentials and their source localization in Attention Network Test. Sci Rep 9(1):1–13

Vázquez-Marrufo M, Galvao-Carmona A, González-Rosa JJ, Hidalgo-Muñoz AR, Borges M, Ruiz-Peña JL, Izquierdo G (2014) Neural correlates of alerting and orienting impairment in multiple sclerosis patients. PLoS ONE 9(5):e97226

Wang X, Ding M (2011) Relation between P300 and event-related theta-band synchronization: a single-trial analysis. Clin Neurophysiol 122(5):916–924. https://doi.org/10.1016/j.clinph.2010.09.011

Williams RS, Biel AL, Wegier P, Lapp LK, Dyson BJ, Spaniol J (2016) Age differences in the attention network test: evidence from behavior and event-related potentials. Brain Cogn 102:65–79

Xue X-J, Su R, Li Z-F, Bu X-O, Dang P, Yu S-F, Liu M (2022) Oxygen metabolism-induced stress response underlies heart–brain interaction governing human consciousness-breaking and attention. Neurosci Bull 38(2):166–180

Yang T, Xiang L (2019) Executive control dysfunction in subclinical depressive undergraduates: evidence from the Attention Network Test. J Affect Disord 245:130–139

Zhang D, Zhang X, Ma H, Wang Y, Ma H, Liu M (2018) Competition among the attentional networks due to resource reduction in Tibetan indigenous residents: evidence from event-related potentials. Sci Rep 8(1):1–10

Zhang M, Gong X, Jia J, Wang X (2021) Unpleasant odors affect alerting attention in young men: an event-related potential study using the attention network test. Front Neurosci 15